Acta Polytechnica CTU Proceedings **42**:67–71, 2023
https://doi.org/10.14311/APP.2023.42.0067

ANALYSIS OF PEEL AND SHEAR STRAINS IN CRACKED LAP SHEAR SPECIMENS SUBJECTED TO FATIGUE LOADING USING DIGITAL IMAGE CORRELATION

Alessandra Panerai*, Gianmarco Piccoli, Luca Michele Martulli, Andrea Bernasconi, Michele Carboni

Politecnico di Milano, Department of Mechanical Engineering, via la Masa 1, 20156 Milano, Italy

* corresponding author: alessandra.panerai@polimi.it

Abstract. Adhesive bonding presents many advantages, such as efficient manufacturing and improved structural performance [1]. However, in structures subjected to fatigue, cracks might initiate and propagate in joints, leading to in-service failure [2]. Most adhesively bonded joints are subjected to combination of peel and shear loads, so mixed I+II mode loading conditions are present [3]. In this work, Cracked Lap Shear specimens, which feature mixed I+II mode loading conditions, were tested under fatigue loading. During tests, crack growth was monitored using Visual Testing and Digital Image Correlation. With Digital Image Correlation, opening and sliding displacements in the bondline were extracted from the substrates' displacement fields and compared against a Finite Element Model, revealing a highly strained process zone ahead of the crack tip. Results highlight the usefulness of DIC in capturing the deformation behaviour of adhesive joints under mixed mode loading conditions.

Keywords: Adhesively bonded joints, cracked lap shear specimen, fatigue loading, digital image correlation.

1. Introduction

In recent years, there has been an increasing interest in the use of adhesive bonding for manufacturing joints. When compared to mechanically fastened joints, bonded joints can offer reduced stress concentrations, easier manufacturing, reduced weight, and improved durability [1]. Adhesively bonded joints have however the issue of reliability because they can present defects coming from manufacturing or initiating during service, which can lead to failure [2]. The ability to detect and locate these defects is crucial for increasing overall safety. Fracture in an adhesively bonded joint is usually a mixed-mode problem, as shear and peel stresses are generally both present in an adhesive layer [3]. To monitor crack propagation, Visual Testing (VT) is the standard technique, but many studies have used Digital Image Correlation (DIC) to monitor crack propagation in either mode I or mode II [4, 5], but only few under mixed mode loading [6].

In this work, we conducted experiments using Cracked Lap Shear specimens subjected to fatigue loading, representing a mixed I+II mode loading condition. Crack growth was monitored using Visual Testing and Digital Image Correlation. DIC results were compared against a Finite Element Model. The results highlight the efficacy of DIC in accurately capturing the deformation behaviour of adhesively bonded joints under mixed mode loading conditions.

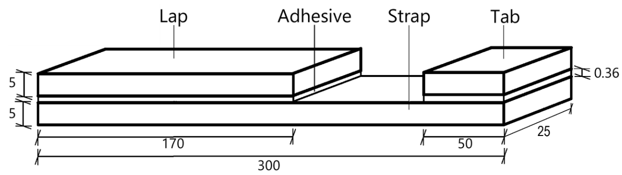

Figure 1. Specimen dimensions.

2. Materials and methods

The CLS specimens were fabricated using 5 mm thick high strength AISI A514 stainless steel plates. Two different types of adhesives were used for bonding: 3M DP490 for specimens 1–4 [7] and 3M 9323 for specimen 5 [8]. The dimensions of the specimens are illustrated in Figure 1.

To create a 10 mm precrack, Teflon strips with a thickness of 0.36 mm were applied to both substrates, ensuring a uniform bondline thickness. Additionally, 1 % by weight of glass microspheres with a diameter of 0.36 mm were added to the 9 323 adhesive to maintain the desired thickness. After clamping, the specimens were cured in an oven at 65° for a minimum of 2 h. One side of the specimens was painted with white brittle paint for visual testing, while the other side was painted with white paint and then with black speckles for DIC monitoring. DIC pictures were taken using a 26.2 Megapixel Canon EOS-RP camera equipped with a Canon RF 85 mm F2 macro IS lens. VT pictures were taken with a 16 Megapixel phone camera.

Fatigue tests were conducted on the specimens using an MTS 370 servo-hydraulic testing machine equipped with a 100 kN load cell (Figure 2). The tests were

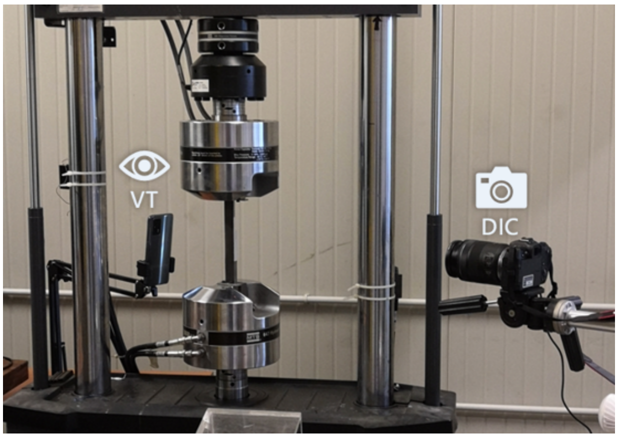

FIGURE 2. Experimental setup.

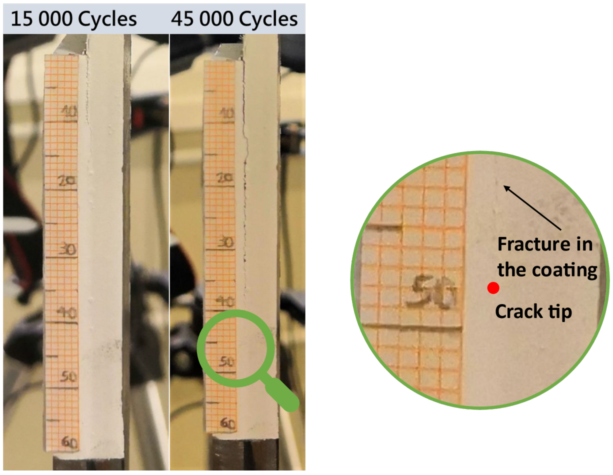

FIGURE 3. Visual testing of specimen 1 at 15 000 and 45 000 cycles. Pictures are taken at the maximum fatigue load (20 kN).

performed with a maximum load of 20 kN and a load ratio of 0.1. At regular intervals, the tests were briefly paused, and the specimen was brought to its maximum load to acquire DIC images and perform VT. A DIC picture was also taken before the fatigue test started at maximum load. In this acquisition (referred as "0 Cycles" in the rest of the article) the crack length is known to be the length of the Teflon insert, as no propagation has occurred, so it was used as a reference for validating the FEM model.

DIC images were post-processed using GOM Correlate 2020. 3-dimensional Finite Element Models of the CLS specimens were created with Abaqus FEA 2022 software considering three different crack lengths, 10, 25, and 30 mm. The models use quadratic elements and reduced integration. Both the steel substrates and the two adhesives were modelled as linear-elastic materials. The elastic moduli were 260 000 MPa for the steel, 1 730 MPa for the DP490 [7] and 2600 MPa for the 9 323 [8]. The adhesive-strap, adhesive-lap, as well as the tab-strap interfaces were modelled by tie constraints.

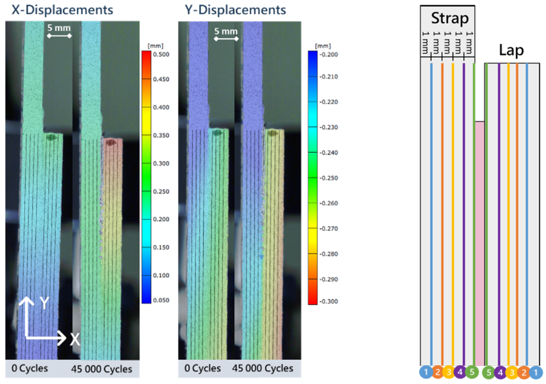

(A). (B).

FIGURE 4. (A) X and Y displacement fields of specimen 1 at 0 and 45 000 cycles; (B) Reference lines from which the displacement values were extracted.

3. Results and Discussion

Visual Testing is commonly used for crack monitoring in mode I loading conditions where the crack tip is easily visible thanks to the opening of the crack. In mode II loading, identifying the exact crack tip position is more challenging. In our mixed-mode setup, although it is evident that crack propagation is occurring, the predominance of mode II loading makes it difficult to precisely pinpoint the crack tip position (see Figure 3).

To overcome this limitation, Digital Image Correlation was used to measure the displacement fields in both X and Y directions (Figure 4). X-displacements can provide insights about mode I behaviour, while Y-displacements can offer information about mode II.

The significant variation in Y-displacements across the thickness of each substrate (Figure 4a) indicates significant shear deformation in the adherends. As fatigue crack growth progresses, the variation in joint stiffness leads to changes in the displacement fields. The displacement values were extracted from parallel lines along the substrates, as illustrated in Figure 4b. Figure 5a demonstrates the change in displacements between 0 and 45 000 cycles for specimen 1.

Analysing the X-displacements reveals that, as fatigue progresses, the separation between lap and strap increases (Figure 5a). The opening (i.e., mode I) displacement in the bondline was obtained from the difference between the mean displacement in each substrate. All five specimens exhibit similar trends, which align with the finite element model (Figure 5b). A few millimetres ahead of the crack tip the opening displacement becomes negative, which is indicative of compressive stresses resulting from bending of the substrates [9]. FEM results show that as the crack length increases, the trend remains similar, but is shifted to the right (Figure 6a). A similar shift is observed in the experimental results (Figure 6b). To monitor crack propagation, two reference points were established: the 0-opening point, where opening displacement was equal to 0, and the position of the

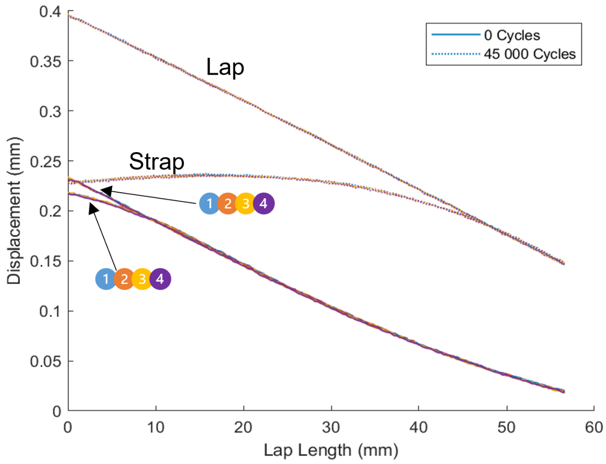

(A). X displacements

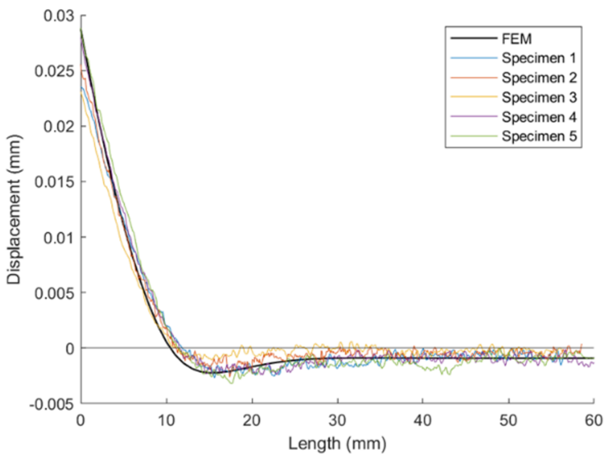

(B). Opening Displacement in the Bondline, 0 Cycles, Crack length 10 mm

Figure 5. (A) X-Displacements of specimen 1 at 0 and 45 000 cycles; (B) Opening displacement in the bondline for all specimens at 0 cycles.

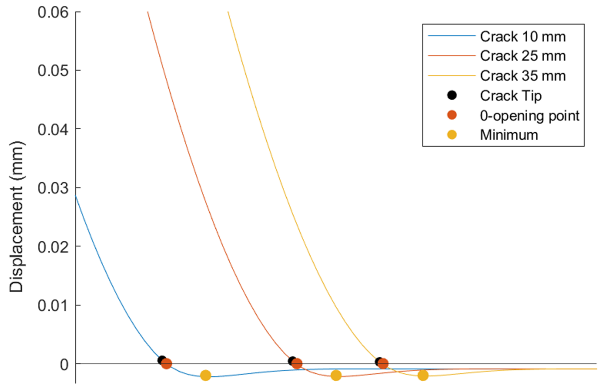

(A). Bondline Opening Displacement

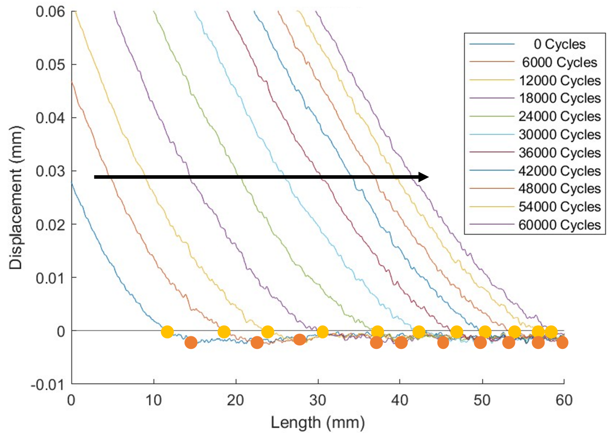

(B). Opening Displacement, Specimen 1

Figure 6. (A) Bondline opening displacement for three different crack lengths obtained by FEM; (B) Evolution of the bondline opening displacement during fatigue of specimen 1 obtained by DIC.

minimum displacement. The two points are shown in Figure 6.

While X-displacements are virtually constant across the thickness of each adherend (Figure 5a), Y-displacements vary significantly (Figure 7a) due to the shear deformation in the substrates. For this reason, taking the difference between the mean displacement in each substrate,as done for the opening displacement, would not be representative of the displacement at the bondline (i.e., between lines 5 in Figure 4b). The sliding (mode II) displacement in the bondline was instead estimated by linearly extrapolating the displacements in each substrate, as shown in Figure 7b. Once again, the five specimens and the FEM show very similar results (Figure 7c), and as the crack length increases, the trend is replicated but shifted to the right (Figures 8a and 8b). In the cracked part of the specimen the sliding displacement shows a linear trend, while in the bonded area far away from the crack tip, the sliding displacement is small and almost constant. Between these two regions, a nonlinear trend is observed. To monitor crack propagation, a linear regression was performed in the linear part of the trend, and the point of deviation from linearity was established as a reference point (Figure 8).

Figure 9 compares the crack length estimations obtained experimentally from Digital Image Correlation and Visual Testing for all specimens, and numerically from the Finite Element Models. Crack length estimations are plotted against the 0-opening point of each acquisition.

The reference points derived from both FEM and DIC are very consistent with each other. FEM results suggests that the 0-opening point is the closest one to the real crack position, while both the minimum opening displacement and the point of non-linearity are a few millimiters further away (i.e., they indicate a longer crack length). However, the distance between the different reference points remains almost constant for all crack lengths considered, so they still provide a reliable, albeit slightly conservative, estimation of crack length. On the other hand, Visual Testing con-

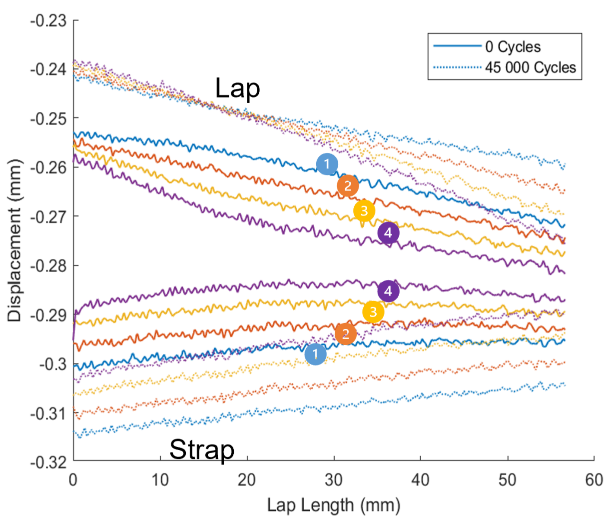

(A). Y displacements

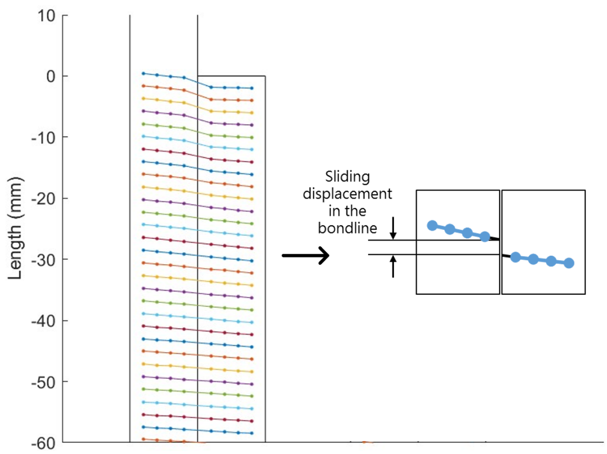

(B). Sliding Displacement

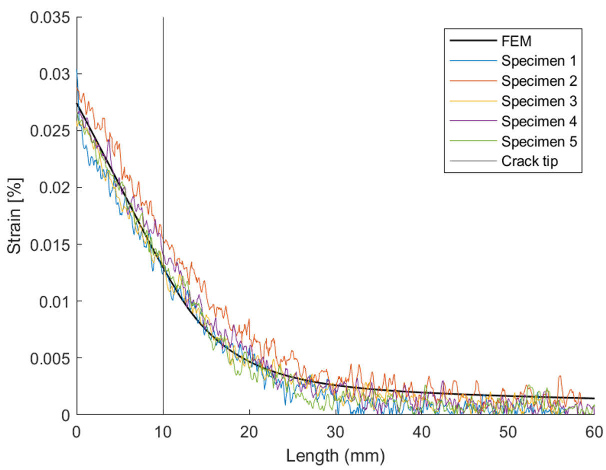

(C). Sliding Displacement in the Bondline, 0 Cycles, Crack length 10 mm

FIGURE 7. (A) Y-Displacements of specimen 1 at 0 and 45 000 cycles; (B) How the bondline sliding displacement was obtained; (C) Sliding displacement in the bondline.

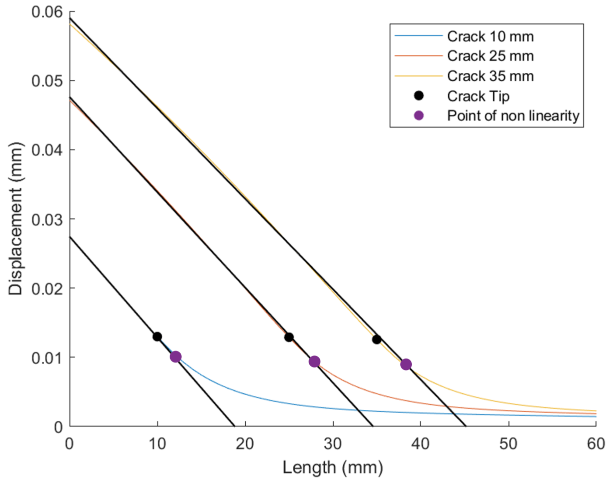

(A). Bondline Sliding Displacement

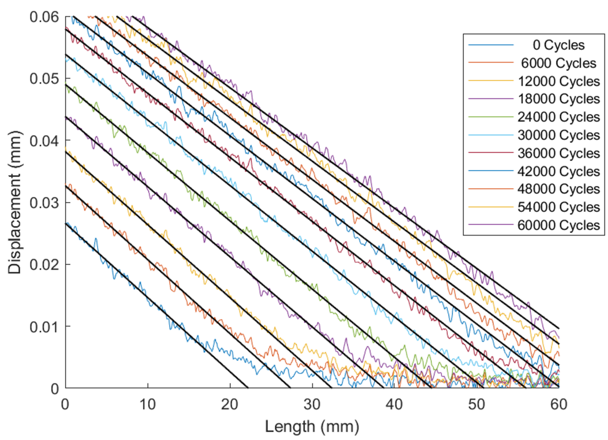

(B). Bondline Sliding Displacement, Specimen 1

FIGURE 8. (A) Bondline sliding displacement for three different crack lengths obtained by FEM; (B) Evolution of the bondline sliding displacement during fatigue of specimen 1 obtained by DIC

sistently underestimates crack length when compared to DIC, and as the fatigue test progresses, this disparity between VT and the other methods becomes more pronounced. This difference is likely due to the predominance of mode II loading, which makes identifying the exact crack tip location difficult.

4. Conclusions

Fatigue tests were conducted on CLS specimens to investigate the effectiveness of DIC and VT in locating and monitoring the crack tip position.

Digital Image Correlation allowed for effective monitoring of crack propagation in adhesive bonded joints under mixed-mode loading conditions.

Using Digital Image Correlation, the opening and sliding displacements in the bondline were obtained from the displacements of the substrates. Good agreement was found between the displacements obtained by Finite Element Modelling and DIC.

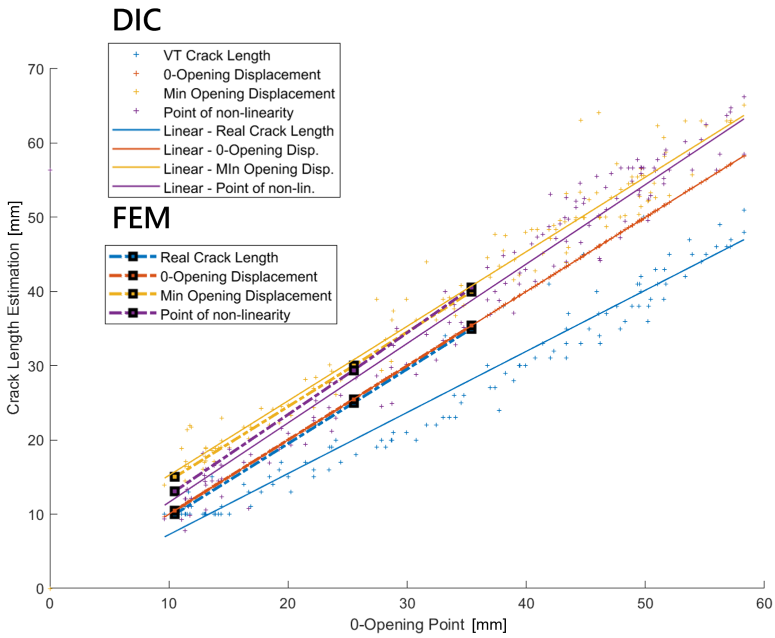

Figure 9. Experimental and Numerical crack length estimations plotted against the 0-opening point for all five specimens.

On the other hand, it was found that identifying the exact location of the crack tip with VT was quite challenging due to the predominance of mode II loading. Additionally, VT measurements consistently yielded lower values than DIC measurements, indicating potential limitations for VT in mixed-mode loading conditions.

References

[1] M. D. Banea, L. F. D. Silva. Adhesively bonded joints in composite materials: An overview. *Proceedings of the Institution of Mechanical Engineers, Part L: Journal of Materials: Design and Applications* **223**(1):1–18, 2009. https://doi.org/10.1243/14644207JMDA219

[2] M. K. Budzik, M. Wolfahrt, P. Reis, et al. Testing mechanical performance of adhesively bonded composite joints in engineering applications: an overview. *Journal of Adhesion* **98**(14):2133–2209, 2022. https://doi.org/10.1080/00218464.2021.1953479

[3] L. Tong, Q. Luo. Analysis of cracked lap shear (CLS) joints. *Modeling of Adhesively Bonded Joints* pp. 25–51, 2008. https://doi.org/10.1007/978-3-540-79056-3_2

[4] M. Zhu, L. Gorbatikh, S. Fonteyn, et al. Digital image correlation assisted characterization of Mode I fatigue delamination in composites. *Composite Structures* **253**:112746, 2020. https://doi.org/10.1016/j.compstruct.2020.112746

[5] O. Orell, J. Jokinen, M. Kanerva. Use of DIC in the characterisation of mode II crack propagation in adhesive fatigue testing. *International Journal of Adhesion and Adhesives* **122**:103332, 2023. https://doi.org/10.1016/j.ijadhadh.2023.103332

[6] F. Ramezani, M. R. Ayatollahi, A. Akhavan-Safar, L. F. M. da Silva. A comprehensive experimental study on bi-adhesive single lap joints using DIC technique. *International Journal of Adhesion and Adhesives* **102**:102674, 2020. https://doi.org/10.1016/j.ijadhadh.2020.102674

[7] 3M™ Scotch-Weld™ EPX™ Adhesive DP490. [2023-06-30]. https://www.3m.co.uk/3M/en_GB/p/d/b40066473/

[8] 3M™ Scotch-Weld™ Structural Epoxy Adhesive EC-9323 B/A, 2022. [2023-06-30]. https://www.3m.com/sds

[9] Q. Luo, L. Tong. Fully-coupled nonlinear analysis of single lap adhesive joints. *International Journal of Solids and Structures* **44**(7-8):2349–2370, 2007. https://doi.org/10.1016/J.IJSOLSTR.2006.07.009